Title

Comparison between inferior frontal gyrus intrinsic connectivity network and verb-generation task fMRI network for presurgical language mapping in healthy controls and in glioma patients

Journal
Brain Imaging and Behavior, 16(6)

ISSN
1931-7557

Authors
Cirillo, Sara
Battistella, Giovanni
Castellano, Antonella
et al.

Publication Date
2022-12-01

DOI
10.1007/s11682-022-00712-y

Peer reviewed

Published in final edited form as:

Brain Imaging Behav. 2022 December ; 16(6): 2569–2585. doi:10.1007/s11682-022-00712-y.

Comparison between inferior frontal gyrus intrinsic connectivity network and verb-generation task fMRI network for presurgical language mapping in healthy controls and in glioma patients

Sara Cirillo[1], **Giovanni Battistella**[2], **Antonella Castellano**[1,3], **Francesco Sanvito**[3], **Antonella Iadanza**[1], **Michele Bailo**[4,3], **Raffaella Lina Barzaghi**[4], **Stefania Acerno**[4], **Pietro Mortini**[4,3], **Maria Luisa Gorno-Tempini**[2,5], **Maria Luisa Mandelli**[2], **Andrea Falini**[1,3]

[1]Neuroradiology Unit and CERMAC, IRCCS Ospedale San Raffaele, Milan, Italy

[2]Memory and Aging Center, Department of Neurology, University of California, San Francisco, CA, USA

[3]Vita-Salute San Raffaele University, Milan, Italy

[4]Neurosurgery and Gamma Knife Radiosurgery Unit, IRCCS Ospedale San Raffaele, Milan, Italy

[5]Department of Psychiatry and Behavioral Science, and Weill Institute for Neurosciences, UCSF, San Francisco, CA 94158, USA

Abstract

Task-based functional MRI (tb-fMRI) represents an extremely valuable approach for the identification of language eloquent regions for presurgical mapping in patients with brain tumors. However, its routinely application is limited by patient-related factors, such as cognitive disability and difficulty in coping with long-time acquisitions, and by technical factors, such as lack of equipment availability for stimuli delivery. Resting-state fMRI (rs-fMRI) instead, allows the identification of distinct language networks in a 10-min acquisition without the need of performing active tasks and using specific equipment. Therefore, to test the feasibility of rs-fMRI as a preoperative mapping tool, we reconstructed a lexico-semantic intrinsic connectivity network

✉ Antonella Castellano castellano.antonella@hsr.it, Giovanni Battistella gvn.battistella@gmail.com.
Sara Cirillo and Giovanni Battistella share first authorship.
Andrea Falini and Maria Luisa Mandelli share last authorship.

Authors contributions SC: data acquisition and analysis, study design and data interpretation. GB: data analysis, study design and data interpretation. AC: data acquisition, study design and data interpretation. FS: data analysis and interpretation. AI: data acquisition. MB, RLB, SA, PM: collection of clinical/neurosurgical data, data interpretation. MLGT, MLM, AF: conception and study design, data interpretation.

Declarations

Competing interests None of the authors have a conflict of interest to declare.

Ethical approval All procedures performed involving human participants were reviewed and approved by Local ethical committee of Ospedale San Raffaele, Milan, Italy.

Code availability Not applicable.
The submitted work has not been published previously and is not being considered for publication elsewhere.

Consent to participate All subjects provided signed informed consent prior to MR imaging.

Supplementary Information The online version contains supplementary material available at https://doi.org/10.1007/s11682-022-00712-y.

Consent to publication Not applicable.

(ICN) in healthy controls (HC) and in a case series of patients with gliomas and compared the organization of this language network with the one derived from tb-fMRI in the patient's group. We studied three patients with extra-frontal gliomas who underwent functional mapping with auditory verb-generation (AVG) task and rs-fMRI with a seed in the left inferior frontal gyrus (IFG). First, we identified the functional connected areas to the IFG in HC. We qualitatively compared these areas with those that showed functional activation in AVG task derived from Neurosynth meta-analysis. Last, in each patient we performed single-subject analyses both for rs- and tb-fMRI, and we evaluated the spatial overlap between the two approaches. In HC, the IFG-ICN network showed a predominant left fronto-temporal functional connectivity in regions overlapping with the AVG network derived from a meta-analysis. In two patients, rs- and tb-fMRI showed comparable patterns of activation in left fronto-temporal regions, with different levels of contralateral activations. The third patient could not accomplish the AVG task and thus it was not possible to make any comparison with the ICN. However, in this patient, task-free approach disclosed a consistent network of fronto-temporal regions as in HC, and additional parietal regions. Our preliminary findings support the value of rs-fMRI approach for presurgical mapping, particularly for identifying left fronto-temporal core language-related areas in glioma patients. In a preoperative setting, rs-fMRI approach could represent a powerful tool for the identification of eloquent language areas, especially in patients with language or cognitive impairments.

Keywords

Resting-state fMRI; Glioma; Language; Task-based fMRI; Seed-based functional connectivity

Introduction

For the presurgical assessment of the language function, the use of multiple paradigms performed with task-based functional magnetic resonance imaging (tb-fMRI) is strongly recommended to increase the sensitivity and specificity of the localization of eloquent cortical areas (Black et al., 2017). Several distributed brain networks underpin specific and interconnected language processes (i.e. semantic, syntax, etc.) and, for this reason, different stimuli are needed to obtain a comprehensive mapping of the areas associated to language functions (Price, 2012). Therefore, this mapping requires long scanning time and, for some patients, it could be a challenge because of their language or cognitive impairments (Antonsson et al., 2018; Noll et al., 2016). These deficits, as well as task complexity are acknowledged as the main factors affecting performance accuracy, even for healthy subjects (Lopes et al., 2016; Weber et al., 2006). Nevertheless, a further aspect that makes tb-fMRI mapping demanding includes the availability of MRI-compatible technical equipment for stimuli delivery. In the context of preoperative evaluation of patients with brain tumors, the use of an fMRI sequence to identify networks of interest without the requirement of neither a cognitive task nor specialized equipment would be able to overcome the limitations mentioned above (Azad & Duffau, 2020; Silva et al., 2018; Sunaert, 2006). Unlike tb-fMRI, resting-state fMRI (rs-fMRI) has the potential to extract multiple linguistically relevant networks within 8/10-min of acquisition while the patient stays still in the scanner without performing any cognitive task (D. M. Cole et al., 2010). This emerging approach is desirable for presurgical mapping, particularly for patients who may have difficulty with task instructions and/or with profound language and cognitive impairments, and available even outside specialized research centers. Although the potential of resting-state technique is to guide the neurosurgeon to preserve eloquent cortical areas during surgery, it is still not used very much in the clinical setting.

Seed-based connectivity analysis (SCA) is a method able to extract functional networks associated to specific cognitive processes from rs-fMRI data by calculating the correlation between the average time-course from a seed region and the time-course from all other voxels in the brain (Biswal et al., 1997; Buckner & Vincent 2007; van den Heuvel & Hulshoff Pol, 2010). As a strong a-priori hypothesis about the seed regions to use for the identification of language-related connectivity networks exists, this method appears to be well-suited in the presurgical mapping of language. Furthermore, SCA results are easier to interpret than those derived from data-driven methods, such as the Independent Component Analysis (ICA). In this study, the use of a SCA is driven by the clinical need of having a fast and easy tool to apply at a single subject level to those patients with linguistic or cognitive deficits who cannot perform properly tb-fMRI.

Among several language tb-fMRI paradigms, the Verb Generation (VG) task is one of the most commonly used and reliable presurgical paradigms for mapping lexico-semantic cortical areas in frontal and temporal lobes. In this task, the retrieval of semantic knowledge and the selection of lexical information among competing alternatives are crucial cognitive processes. During this paradigm, several nouns are presented to the participant, and for each of them the participant needs to silently think of a verb semantically related to that given noun, for example “bark” in response to “dog”. To adequately perform the task, the subject has to access the semantic knowledge and to choose the appropriate verb in response to the presented noun.

As shown in previous studies on healthy controls (HC), this task activates a network that encompasses distributed language areas predominantly in left fronto-temporal regions, such as the inferior frontal gyrus (IFG) and the middle and superior temporal gyri (Allendorfer et al., 2012; Cerliani et al., 2017; Grezes & Decety, 2001). This well-established topographical organization of the lexico-semantic network is also reported in fMRI-based meta-analytic tools, such as Neurosynth, which is able to collect from the literature all previous works related to VG activation network.

Few rs-fMRI studies in HC have investigated specific language networks such as the lexico-semantic one, and they showed a pattern of fronto-temporal regions similar to those activated in the VG task using a seed in Broca’s area (Battistella et al., 2020; Muller & Meyer, 2014; Smitha et al., 2017; Tomasi & Volkow, 2012; Zhu et al., 2014).

However, the capability of rs-fMRI to identify language eloquent cortex compared to tb-fMRI has yet to be fully understood both in healthy population and in patients with brain tumors. To our knowledge, only few ICA-based studies compared language rs-fMRI maps and task-specific fMRI activations in brain tumors’ patients, reporting a good level of spatial overlap between these two approaches (Branco et al., 2016; Lu et al., 2017; Sair et al., 2016).

This study aims at testing the potential feasibility of preoperative evaluations based on rs-fMRI compared to conventional tb-fMRI protocol, by comparing the language eloquent areas activated in a standard and reliable verb generation paradigm with a task-free paradigm. We first extracted the intrinsic connectivity network (ICN) from rs-fMRI data in a group of HC by positioning the seed in the left Broca's area (IFG) in order to identify a reference task-free network in the healthy population. We then investigated qualitatively the topographical organization of the regions activated in HC during tasks related to the VG network by using a meta-analytic tool (Neurosynth). Finally, we performed the same rs-fMRI protocol in a case series of presurgical patients with extra-frontal gliomas and compared at a single-subject level the spatial overlap between the regions activated during an auditory VG fMRI task and those activated in rs-fMRI. Our hypothesis is that the spatial correspondence between functional maps obtained with rs-fMRI and tb-fMRI might support the use of task-free paradigms in substitution of task-based multiple paradigms, especially in cases where the participant experiences difficulties with the task and/or is too cognitively impaired.

Materials and methods

Participants

A group of 15 native Italian healthy speakers (5 males, 10 females; age range: 24–64 years; mean age: 35.4 ± 12.7) underwent rs-fMRI at the Neuroradiology Unit and CERMAC, IRCCS Ospedale San Raffaele HSR (Milan, Italy). Healthy controls were all right-handed and none of them was bi- or multilingual. These acquisitions were used to evaluate the language ICN in a healthy population. For this group, tb-fMRI acquisitions were not available, thus we used a meta-analysis platform called Neurosynth in order to identify the regions involved in lexico-semantic processes in the healthy population. These participants did not have a history of neurological disorders and the brain MRI scans presented no abnormalities.

Patients with brain tumors were selected based on the following criteria: a) extra-frontal tumors histopathologically confirmed as brain gliomas; b) referred for language presurgical mapping with AVG paradigm. Patients that presented hydrocephalus and deviations of the cerebral midline that could have heavily distorted gross brain anatomy were excluded. Five patients resulted eligible for the study, as they met the criteria of the study (Table 1). The Karnofsky Performance Status (KPS) scale was administered as an indicator of functionality in everyday life (score range from 0 = worse to 100 = good) (Karnofsky DA, 1949).

All participants were right-handed as determined by the Edinburgh Handedness Inventory test (Oldfield, 1971). Written informed consent was approved by the Internal Review Board at HSR.

MRI acquisition protocol and fMRI language paradigm

MR imaging data were acquired on a 3.0 T Ingenia CX MR scanner (Philips Healthcare, Best, The Netherlands). Conventional MRI protocol included a 3D Fluid Attenuated Inversion Recovery (3D-FLAIR) sequence (TR/TE: 9000/290 ms; flip angle, 40°; voxel size reconstruction: 0.68 × 0.68×0.7 mm^3; FOV, 230 × 221 mm^2; 204 axial slices; slice thickness, 1.2/ −0.5 mm gap; acquisition matrix, 204 × 197; SENSE reduction factor R = 2.5; acquisition time = 7 min 30 s) and a high-resolution volumetric 3D fast field echo (FFE) axial T1-weighted sequence for brain tissue segmentation and registration of functional images (TR/TE 8000/4000 ms; flip angle, 8°; voxel size reconstruction: 0.65 × 0.65×0.8 mm^3; FOV, 260 × 206 mm^2; 207 axial slices; acquisition matrix 260 × 300; SENSE reduction factor, R = 2.2; acquisition time = 4 min 52 s).

Resting-state fMRI task—Functional images with blood oxygen level dependent (BOLD) contrast were obtained with a T2*-weighted single-shot echo-planar imaging (EPI) gradient echo sequence. For rs-fMRI, a total of 290 dynamics were acquired during a 8-min scan with the following parameters: TR/TE, 1700/35 ms; matrix, 96 × 94; FOV, 240 mm; flip angle, 90°; voxel size, 2.5 × 2.5×2.5 mm^3; 52 axial slices; SENSE reduction factor, R = 2; dummy scans = 5; phase-encoding direction, anterior-to-posterior. Participants were instructed to stay still and to keep their eyes closed without falling asleep during the acquisition of the rs-fMRI data. An extra volume for susceptibility distortion correction of the functional images was also acquired using the same parameters in opposite phase encoding direction (posterior-to-anterior)

VG-fMRI task—For the VG fMRI task, a total of 100 dynamics were acquired during a 6-min scan with the following parameters: TR/TE = 3700/30 ms; matrix, 128 × 128; FOV, 240 mm; flip angle, 85°; voxel size, 2 × 2 × 4 mm^3; 32 axial slices; SENSE factor, R = 2; dummy scan = 2. During the VG task, patients performed a block-designed lexico-semantic retrieval verb-generation task, with 10 blocks of activity of 22 s each alternated with 10 blocks of control condition of 14 s each. The noun-to-verb generation is a well-established paradigm to investigate lexico-semantic processes (Benson et al., 1999; Petersen et al., 1988) (Sanvito et al., 2020), based on the original task introduced by Petersen et al., (Petersen et al., 1988). For a given noun presented in an auditory form, subjects had to silently generate a semantically related verb (i. e. ‘to read’ when the subject hears the noun ‘book’). The nouns used were sorted among nouns with a clear dominant response i.e. “scissor” – “to cut” as reported in a previous fMRI investigation (Thompson-Schill et al., 1997). The control condition consists of counting from 0 to 10. The task was performed sub-vocally to prevent from motion artifacts and speech-associated activation of primary motor and somatosensory areas. Prior to the scanning session, patients executed a brief overt version of the VG task to ensure a full understanding and a correct performance of the task. The nouns were different compared to the in-scanner version but with comparable level of difficulty.

Clinical history and neuroradiological description of the case studies

Case 1—A 44-year-old female presented with a left parietal oligodendroglioma (WHO, II) involving the superior parietal cortex and the underlying subcortical white matter, and extending to the paracentral lobule (Fig. 1A) and angular gyrus. Clinical onset was characterized by loss of right arm and leg sensitivity without any language deficits. KPS score was 100 preoperatively and remained stable postoperatively.

Case 2—A 46-year-old male presented with a left temporal anaplastic astrocytoma (WHO, III), involving multifocal lesions within the middle temporal gyrus and mesial occipito-temporal regions (Fig. 1B). Clinical onset was characterized by generalized seizures and language deficits. KPS score was 100 preoperatively and worsened postoperatively to a score of 80.

Case 3—A 34-year-old female presented with a left ganglioglioma (WHO, I), involving the left mesial temporal lobe (Fig. 1C). Clinical history of the patient was characterized by severe and drug-resistant epilepsy since childhood, and language deficits. KPS score was 100 preoperatively and remained stable postoperatively.

Case 4—A 48-year-old male presented with a left oligodendroglioma (WHO, III), involving the whole left temporal lobe (Fig. 1D). Clinical history of the patient was characterized by memory deficit (short-term amnesia) and paresthesia felt to the right side of the body, without any language deficits. KPS score was 100 preoperatively and remained stable postoperatively.

Case 5—A 69-year-old male presented with a left glioblastoma (WHO, IV), involving the left mesial temporal lobe (Fig. 1E). Clinical history of the patient was characterized by spatial–temporal disorientation and language deficits (at MR scan the patient did not present any language deficits). KPS score was 100 preoperatively and remained stable postoperatively.

Functional MRI data preprocessing

Pre-processing of the functional MRI data were performed using the Oxford Centre for Functional Magnetic Resonance Imaging of the Brain Software Library (FMRIB, Oxford UK; FSL version 5.0.11), Statistical Parametric Mapping, SPM12 software (http://www.fil.ion.ucl.ac.uk/spm) implemented in Matlab (MATLAB R 2017a, The MathWorks Inc.), and Conn toolbox 17.1 (http://web.mit.edu/swg/software/).

The first 4 functional volumes were discarded to allow steady-state magnetization to be established. The images were then corrected for susceptibility induced distortions, slice-timing corrected and realigned to the average volume. The average functional volume was then used to co-register the fMRI data with the structural T1 image. The T1-weighted structural image was segmented into grey matter (GM), white matter (WM) and cerebrospinal fluid (CSF) using the unified segmentation approach implemented in SPM12 (Ashburner & Friston, 2005) and spatially normalized to Montreal Neuroimaging Institute (MNI) template space. The same deformation of the structural image was applied to the functional images that were then resampled at $2 \times 2{\times}2$ mm^3 and finally smoothed with a Gaussian kernel of 6 mm full-width at half-maximum (FWHM). For each participant, results from the normalization step were carefully visually inspected. Of note, none of the patients presented a tumor lesion with mass effect.

IFG seed-based functional connectivity analysis

A seed-based correlation analysis (SCA) on rs-fMRI data using a region of interest (ROI) in the left IFG was performed in both HC and patients. As our interest was to identify an ICN related to lexico-semantic processing, the seed-ROI was defined in the triangular portion of the inferior frontal gyrus (triIFG). This a priori seed-ROI was defined according to the well-known functional contributions of this area to lexico-semantic processing. IFG, and specially its anterior portion, the pars triangularis, is involved in retrieval of verbal information in the language-dominant hemisphere and more generally in semantic processing (Price, 2012; Saur et al., 2008).

The ROI was created in the MNI space as a sphere of 5 mm of radius centered in $x = -56$, $y = 24$, $z = 15$ with Mars-Bar SPM toolbox (Fig. 3) (Brett et al., 2002). These coordinates were derived from two rs-fMRI studies investigating intrinsic language networks using the same seed (Friederici et al., 2011; Muller & Meyer, 2014). Since the coordinates in the abovementioned studies were reported in Talairach space (x −53, y 20, z 15), we transformed them in the MNI space for our study.

The correct localization of the ROI after the normalization of the functional volumes was verified for each subject, in particular in the patients' cohort where the presence of the tumor could lead to normalization errors. This ROI was used for seed-based whole-brain correlational analysis to identify the language-related resting-state intrinsic networks. The analyses were performed with the Conn Toolbox (version 17) (http://web.mit.edu/swg/software/) in SPM (Whitfield-Gabrieli & Nieto-Castanon, 2012). The steps for the pre-processing were the following: i) linear regression of confounding factors including WM and CSF signals (5 components each), motion parameters (6 motion parameters and 6 first-order temporal derivatives of the associated time series) by using the CompCor removal method (Behzadi et al., 2007), ii) band-pass filtering (0.008–0.1 Hz) (Cordes et al., 2001), and iii) linear detrending and despiking after regression to remove linear drift artifacts and secondary movement-related artifacts (Patel et al., 2014).

The inferior frontal gyrus intrinsic connectivity network (IFG-ICN) was calculated with a seed-to-voxel analysis using a weighted general linear model (GLM). Correlation maps were generated by computing the correlation coefficients (r) between the average BOLD signal time-course from the seed and the time-course from all the other voxels in the brain.

In the HC group, functional connectivity correlation maps were converted to z scores by Fisher's r-to-z transformation and submitted to one-sample t-test (using age and sex as regressors of no interest) to compute the group-level intrinsic connectivity map derived from the left IFG seed. Results were assessed at p-value < 0.0001 uncorrected (cluster extent $k = 40$). The anatomical distributions of the significant clusters are reported based on standard atlas of cortical areas (Tzourio-Mazoyer et al., 2002), available with the SPM software package.

In patients, functional connectivity correlation maps were obtained at single-subject level. First-level covariates included the motion parameters of each patient. The correlation thresholds were set at a correlation coefficient of r = 0.3, $p < 0.05$, as estimated in the first level analysis of the CONN pipeline.

Neurosynth meta-analysis for AVG task-based fMRI in healthy controls

Since tb-fMRI was not acquired in HC, we performed a meta-analysis using Neurosynth —a publicly available platform (http://Neurosynth.org)—with the only aim of obtaining a reference network associated to tb-fMRI verb generation paradigms in the healthy population. VG network derived from Neurosynth platform was only used for descriptive purpose and no formal quantitative overlap analysis was conducted because of the intrinsic limitation of Neurosynth related to the impossibility to control for specific experimental factors in each of the studies included in the meta-analysis. Neurosynth automatically synthesizes the results of large-scale different fMRI data in a meta-analytic approach. Its utility here is exploited for a qualitative large-scale analysis involving a broad linguistic domain ("verb-generation").

The database contained 14,371 studies and 1,335 terms for meta-analysis searches when interrogated on 22th of May 2019 (Yarkoni et al., 2011). The Neurosynth platform was interrogated for the term "verb" for VG task. This search produced a list of 127 fMRI studies that contain this term and the fMRI activation associated map. Neurosynth functional map was provided in the standard 2 mm MNI template space and the threshold was set at $p < 0.01$, false discovery rate (FDR) corrected.

AVG task-based fMRI analysis in patients

Task-based functional tasks data were acquired only in patients. The task-based functional data were analyzed using a whole-brain univariate GLM according to our specific block design experiment. Statistical parametric maps of the contrasts of interest were computed for each subject modelling the active and the passive blocks. The hemodynamic responses induced by task trials were convolved with a hemodynamic response function. To correct for residual head motion, the six realignment parameters were included in the design matrix as regressors of no interest. A high-pass filter of 128 s was applied to remove slow signal drift. These steps resulted in whole brain individual beta-maps containing the regression coefficients for each voxel and the corresponding standard deviations of the beta-values. Single-subject activation maps were thresholded at $p < 0.05$ FWE corrected and cluster extent of 30 voxels.

Spatial overlap analysis of the language network between resting-state and task-based fMRI in patients

We compared the activations derived from rs-fMRI and tb-fMRI in patients by evaluating the degree of overlap between the IFG-derived intrinsic network map and AVG activation map in each patient. As the typical AVG activations mainly comprised left frontal (IFG) and temporal regions (middle and superior temporal gyrus), we restricted the calculation of the overlap to only these left-lateralized language-relevant areas (Allendorfer et al., 2012; Berlingeri et al., 2008; Grezes & Decety, 2001; Sanjuan et al., 2010). The ROIs were created using the probabilistic cortical and subcortical Harvard–Oxford Atlas available in FSL (http://fsl.fmrib.ox.ac.uk/fsl/fslwiki/Atlases) by merging the pars opercularis and triangularis for the frontal ROI and the middle and superior temporal gyri for the temporal ROI, at a probability of 90%. This threshold was chosen based on a visual inspection that showed an accurate correspondence with the anatomical landmarks (Fig. 2).

The IFG-ICN and AVG tb-fMRI networks were thresholded *($r = 0.3$, $p < 0.05$ for rs-fMRI, $p < 0.05$ FWE corrected, cluster extent of 30 voxels for tb-fMRI)*, and then binarized and masked with the two frontal and temporal ROIs. We calculated the percentage of overlapping voxels in each of the language ROIs as follows:

$$\% = \frac{number\ of\ voxels\ in\ the\ intersection\ of\ masked\ tb\ and\ rs}{number\ of\ voxels\ of\ masked\ tb}$$

Results

Resting-state fMRI: healthy controls and patients with brain tumors

Brain areas showing positive correlation with the left IFG in HC are shown in Fig. 3A and listed in Table 2. Specifically, the left IFG significantly correlated in the frontal lobe with bilateral IFG (pars triangularis), left premotor area, left supplementary motor area (SMA) and pre-supplementary motor area (pre-SMA) as well as in the temporal lobe with left superior temporal gyrus (STG), middle temporal gyrus (MTG), inferior temporal-occipital regions and right MTG. Additional clusters were found in the caudate nucleus bilaterally and in the posterior lobe of the right cerebellum (Crus I) *($p < 0.0001$ uncorrected, $T = 4.99$, cluster correction FWE, $k = 40$)*.

Consistently with the results reported in the HC enrolled in this study, the IFG intrinsic connectivity network (IFG-ICN) obtained in glioma patients showed the involvement of frontal and temporal lobes. In patients, the IFG-ICNs globally comprised cortical areas in the left hemisphere in IFG (triangularis and opercularis part), premotor area, SMA and in the posterior part of STG (Fig. 4 and Supplementary Fig. 1). In the right hemisphere, other functionally-connected regions were the triIFG, the premotor area and the cerebellum. In Case #1, the patient presenting with an oligodendroglioma in the left parietal region, the ICN included bilateral IFG and premotor areas, left SMA, posterior part of the left STG and the right cerebellum. In Case #2, the patient presenting with a multifocal anaplastic astrocytoma in the left temporal lobe, the ICN included cortical areas in the left frontal lobe, as well as the STG and MTG of the left hemisphere. Case #3, the patient harboring ganglioglioma in the left temporal pole, showed a bilateral network including frontal and prefrontal regions, and temporo-parietal areas. In Case #4, the patient presenting an oligodendroglioma invading the majority of the left temporal lobe, the ICN included left IFG and SMA, posterior part of STG and MTG, supramarginal gyrus (SMG) and bilateral premotor areas. Case#5, the patient harboring a glioblastoma in the mesial temporal lobe, showed a bilateral network including IFG, SMA and STG, as well as left MTG and SMG.

Task-based fMRI: healthy controls and patients with brain tumors

As expected, functional activations derived from Neurosynth using the keyword “verb” showed a left-lateralized network characterized by the recruitment of opercular and triangular part of IFG, anterior and posterior superior temporal sulcus (STS), STG, MTG as well as SMA and precentral/middle frontal gyrus. In the right hemisphere, insular cortex, middle frontal gyrus (MFG) and posterior cerebellum were also significantly activated *($p < 0.01$, FDR-corrected)* (Fig. 3B).

In patients, the analysis of the AVG task showed statistically significant activations of the main language-related regions in the left hemisphere, including IFG, STG, STS, and SMG *($p < 0.05$, FWE-corrected, cluster extent $k > 30$)* (Fig. 4 and Supplementary Fig. 1) for Case #1, #2, #4 and #5. Case #1, #4 and #5 showed a left-lateralized network of AVG-related activations, while Case #2 activated a bilateral pattern of language areas. On the other hand, Case #3 was not able to correctly perform the AVG task either outside or inside the scanner, because of the severity of language impairments. For this reason, with a FWE-corrected threshold, Case #3 did not show significant activations in the AVG task. However, using a lower threshold (*$p < 0.001$, uncorrected, cluster extent $k > 10$*) small clusters of activations were found in the left hemisphere, particularly in the IFG, inferior temporal gyrus, superior temporal gyrus, and superior parietal lobule. This result should be taken with caution as the statistical significance is relatively low.

Overlap between resting-state and task-based fMRI: patients with brain tumors

Patients showed a percentage of overlap between resting-state and task-based maps superior to 40% in the frontal lobe (Case #1: 803/1390 voxels = 57.77%; Case #2: 916/2075 voxels = 44.14%, Case #4 469/625 voxels = 75.04%, Case #5: 389/948 voxels = 41.03%,) and lower in the temporal regions compared to the frontal ones (Case #1: 92/516 voxels = 17.82%; Case #2: 36/1204 voxels = 2.99%, Case #4: 17/178 voxels = 9.55%, Case #5: 13/109 voxels = 11.92%).

Figure 5 (and Supplementary Fig. 2) illustrates the overlap between the two functional maps in four patients (Case #1, #2, #4, #5). It shows that in the temporal lobe the AVG network recruited a more anterior portion of STG in the proximity of the auditory primary cortex—probably due to the auditory presentation of the stimuli—compared to the IFG-ICN, which instead encompassed mostly posterior portion of STG, MTG, STS and SMG. This different recruitment of temporal lobe areas observed for rs-fMRI and for AVG task might contribute to explain why the overlap between the two networks is higher for the frontal lobe compared to the temporal one. The calculation of the percentage of spatial overlap between rs- and tb-derived maps for each patient was able to give us preliminary information about the ability of the resting-state technique to identify voxels that are significantly activated also in the AVG task.

Discussion

Using seed-based connectivity on rs-fMRI data, we identified a lexico-semantic ICN in HC composed of cortical regions that resembles the topographical organization of the tb-derived AVG activation map, with the highest degree of overlap in frontal regions. These results suggest the functional relevance of the triIFG seed in identifying a relevant language intrinsic network with rs-fMRI technique that could be potentially used in the presurgical mapping of eloquent cortex in patients with brain tumors.

Comparable patterns of intrinsic connectivity and functional activations were found in a case series of patients with left extra-frontal gliomas, with the highest degree of overlap between the two networks observed in the frontal lobe (Case #1, #2, Case #4 and #5).

Despite Case #3 was too impaired to properly perform the AVG task, his rs-fMRI map displayed a bilateral network covering the expected frontal and temporal regions and additional parietal regions.

An extensive discussion about the functional characteristics and possible role of IFG-ICN for preoperative mapping is deepened in the next paragraphs, in the context of language functional connectivity studies and tb-fMRI investigations using VG paradigm in HC and in glioma patients.

IFG resting-state fMRI intrinsic connectivity network in healthy controls

In our study, the pattern of brain regions that are functionally connected to the IFG seed in HC is consistent with recent investigations showing that IFG-seeded rs-fMRI network includes an extended and mostly left-lateralized network of inferior frontal, middle and superior temporal regions (Muller & Meyer, 2014; Smitha et al., 2017; Tomasi & Volkow, 2012; Zhu et al., 2014).

The left frontal and temporal areas identified in the IFG-ICN are associated to lexico-semantic processes and language comprehension, while the left premotor region, SMA, and pre-SMA are involved in motor speech and language production (Price, 2010). In line with former meta-analyses of language-related neuroimaging data, our findings highlight the contribution of the right homologues of both IFG and MTG in lexico-semantic processing (Price, 2012; Vigneau et al., 2011). However, the IFG-ICN is found to be almost leftward lateralized in our HC group. This finding is in correspondence with prior rs-fMRI studies and supported the left hemisphere dominance of a lexico-semantic intrinsic network using a seed in the pars triangularis (Tomasi & Volkow, 2012; Zhu et al., 2014).

Notably, the left premotor area has already been found to be part of the articulation network proposed by Hickock et al., (Hickok & Poeppel, 2007). Also, the functional correlation between left IFG and subcortical structures—such as the caudate nucleus and the cerebellum—in our study is not surprising. In fact, growing evidence points to the involvement of the caudate nucleus in monitoring cognitive processes during language tasks, and of the posterior cerebellar regions in high-level phonological, semantic, and syntactic processing (Crinion et al., 2006; Marien & Beaton, 2014).

IFG resting-state fMRI intrinsic connectivity networks in patients with brain tumors

Until now, to our knowledge, a limited number of reports have investigated the rs-fMRI capability to identify language-related networks in patients with tumors, especially with gliomas. Altogether, these studies were able to detect intrinsic connectivity maps localized in the inferior frontal, superior temporal, dorsolateral prefrontal and supplementary motor cortex of the left hemisphere consistent with our findings (Briganti et al., 2012; Hart et al., 2017; Lu et al., 2017; Metwali & Samii, 2019).

In the present study, in patients with left extra-frontal gliomas, we find a pattern of intrinsic connectivity with similarities and discrepancies to the one observed in HC group. In Case #1, who displayed a parietal oligodendroglioma, in Case #2 presenting with a multifocal temporal anaplastic astrocytoma, and in Case #4 showing a lesion invading the whole temporal lobe, the network is mostly left-lateralized, as described in HC. Conversely, in Case #3 presenting with a ganglioglioma in the temporal pole, and in Case #5, who displayed a glioblastoma, the IFG-ICN encompasses functional areas distributed in both hemispheres such as bilateral temporo-parietal areas.

The spatial organization of the ICNs in the five glioma cases analyzed in our study is consistent with recently published seed-based rs-fMRI studies on seven left-sided glioma patients assessed at the single-subject level, as well as with group findings of left temporal lobe epileptic patients, which both positioned the seed in the left IFG (Doucet et al., 2017; Lu et al., 2017). Despite relying on a different methodology, also the ICA language components extracted in a sample of tumor/epileptic patients by Branco et al., are concordant with our findings (Branco et al., 2016).

Even though Case #3 was too impaired to properly perform the AVG task, the rs-fMRI discloses a language ICN consistent with the one identified in HC for the left frontal and temporal areas. This finding supports the idea that rs-fMRI might represent a powerful technique to identify language-relevant ICNs in cognitively impaired patients. In patients presenting language deficit who cannot perform properly fMRI mapping, as occurred in Case #3, a task-free paradigm can be used as an alternative approach to map language function since it is less demanding. However, in these patients language mapping can be still challenging.

Despite not providing conclusive information regarding the “functionality” of the language cortex, a rs-fMRI mapping might be exploited in the intraoperative phase during awake surgery by guiding the neurosurgeon in the intraoperative direct electrocortical stimulation (DES). Initial evidence supporting the accuracy evaluation between rs-fMRI predictions and DES findings has been reported in the literature (Vakamudi et al., 2020; Cochereau et al., 2016; Zaca et al., 2019). Intraoperative validation represents a necessary step to validate rs-fMRI technique in preoperative setting as previously occurred for task-based fMRI technique (Giussani et al., 2010).

Furthermore, the involvement of additional left parietal areas, as well as right temporo-parietal areas in this patient presenting with language deficits, might suggest that a possible functional reorganization could have occurred. A recent rs-fMRI study using network-based statistics have shown that possible reorganizational mechanisms can underlie different levels of language impairments in patients with gliomas in the left hemisphere (Yuan et al., 2020).

Lastly, although the choice of the seed placement is considered challenging in brains with growing lesions, seed-based correlation analysis appears to be well-suited for the identification of a specific network associated to a distinct language process as opposed to data-driven methods (van den Heuvel & Hulshoff Pol, 2010). In fact, the blind decomposition of the signal through which several independent functional networks are simultaneously extracted in ICA does not allow to easily identifying a specific cognitive process underpinning a broad cognitive domain. Even if the distance between the site of the seed in the triIFG is far from the tumor location to avoid a possible alteration of BOLD signal due to the tumor presence, it cannot be completely ruled out that a functional reshaping occurred at an individual level in the language network.

VG task-based fMRI meta-analysis network in healthy controls

In the present study, the VG functional maps based on the Neurosynth meta-analysis show a strongly left-lateralized network consistent with language areas typically engaged during silent verbalization. Several fMRI studies have already described that the VG is associated with activity of left IFG, MTG and STG, as well as premotor and SMA areas and occasionally the inferior parietal lobule (Allendorfer et al., 2012; Cerliani et al., 2017; Grezes & Decety, 2001; Sanjuan et al., 2010).

In a meta-analysis on the neural networks engaged in the verbalization of actions, pars triangularis and pars opercularis are mainly activated in VG (Grezes & Decety, 2001), as shown in our study. The observed activity in temporal regions is related to the storage and the retrieval of semantic memories (Hickok & Poeppel, 2004; Vigneau et al., 2006). In fact, while left temporal regions are considered to be critical for the semantic store, IFG is thought to regulate the recovery of semantic information, presumably via top-down signals to temporal cortex (Thompson-Schill et al., 1997). In particular, the activation of triIFG is attributable to the process of selection of information from different competing alternatives in the sematic memory, and the difficulty in verb retrieval is correlated with the strength of association between the verb and the noun-cue (Crescentini et al., 2010).

AVG task-based fMRI networks in patients with brain tumors

Our findings related to AVG tb-fMRI networks in patients show commonalities and differences to the ones observed in Neurosynth meta-analysis. In Case #1, #4 and #5, tb-fMRI reveals a predominant left-lateralized network analogous to the map identified in the meta-analysis. In Case #2, tb-fMRI also discloses a more pronounced involvement of the right hemisphere with activations peaks in bilateral IFG and STG. In Case #3, tb-fMRI does not reveal significant brain activations associated with AVG task (using a corrected threshold).

Of note, the presence of the tumors in the temporal lobe could have had an impact on the functional activations in Case #2, #4 and partially in Case #3, who indeed displayed tumors located in temporal regions. In patients with gliomas, atypical distributions of the BOLD response may be considered evidence of brain functional reorganization. Low-grade gliomas are more likely to lead to functional plasticity, according to the observation that slow-growing lesions may induce cerebral reorganization processes because the recruitment mechanism of both ipsilateral and contralateral regions is more efficient (Duffau, 2005) (Cirillo et al., 2019). However, despite suggestive evidence of cortical language rearrangements (Gebska-Kosla et al., 2017; Kosla et al., 2012; Kristo et al., 2015), the association between functional patterns and language deficit recovery in large cohorts of patients has to be further clarified.

Furthermore, the lack of activation in Case #3 could be explained by the suboptimal performance during AVG task, likely due to her significant language impairment already evident at the phonemic fluency test before the MR scan. Although a complete neuropsychological assessment was not achieved in these patients, we hypothesize that the language difficulties showed by Case #3 may explain the poor AVG performance.

It is known that a systematic relation between cortical activation, task performance and task difficulty in language-related paradigms exists in healthy population (Booth et al., 2003; Drager et al., 2004; Fu et al., 2002), as well as in epileptic patients who underwent a presurgical language fMRI mapping (Weber et al., 2006). In the presurgical evaluation of patients with brain infiltrating lesions or with epilepsy, the issue of task performance and task complexity is highly relevant because it has an impact on the reliability of language mapping. To overcome this issue, adaptive fMRI paradigms as described in aphasic patients (Wilson et al., 2018), and online monitor of task performance (Weber et al., 2006) could represent valid tools. However, adaptive tasks are still uncommon in the clinical setting, while the monitoring of performance may request an overt version of the language task.

Finally, VG paradigm was chosen versus other language tb-fMRI paradigms because it is suitable for patients harboring lesions in the temporal lobe since the ultimate goal of presurgical mapping is to localize eloquent perilesional cortical areas. Differently from tb-fMRI VG activation network, the pattern of activations described during a phonemic verbal fluency task in healthy subjects (and anecdotally also in brain tumor patients in our clinical practice) recruits only different portions of left inferior frontal gyrus, middle frontal gyrus and premotor areas (Meinzer et al., 2009). Phonemic fluency paradigm is not able to capture the activation of posterior temporal language areas and consequently comparison between rs-fMRI paradigm and tb-fMRI phonemic fluency task was not taken into account for this study.

Comparison between resting-state and task-based fMRI networks in left frontal and temporal lobe in patients with brain tumors

Previous reports showed that rs-fMRI networks in a healthy population mirror a variety of sensorimotor and cognitive task-based networks suggesting that cognitive-relevant networks can be detectable also with rs-fMRI technique (M. W. Cole et al., 2014; Smith et al., 2009). Recent studies demonstrated the capability of rs-fMRI to identify ICNs involved in several language processes in HC and neurodegenerative patients, and that these networks resembled those activated in tb-fMRI (Battistella et al., 2019, 2020; Lohmann et al., 2010). However, investigations that compared rs-fMRI-derived language networks to tb-fMRI language activations are scarce in brain tumor patients (Branco et al., 2016; Lu et al., 2017; Sair et al., 2016). Although a substantial subject-level variability was reported in these studies, fair to good levels of concordance were found between rs-fMRI and tb-fMRI.

We show that functional brain areas common to rs-fMRI and tb-fMRI have a higher overlap in the regions mostly located in the inferior frontal cortex. The involvement of regions in the IFG (pars triangularis and opercularis) is not surprising, being them well-known functional areas involved in many linguistic and cognitive processes related to language, such as semantic and syntacting processing, speech production, articulatory planning and short-term memory.

In contrast, the percentage overlap between rs-fMRI and tb-fMRI in patients are lower in the temporal lobe. In Case #1 and Case #5, the AVG network includes a more anterior portion of STG, while the IFG-ICN comprises a posterior portion of STG, MTG, STS and SMG. As expected, the AVG task activates also primary auditory areas of STG for the acoustic analysis of the linguistic stimuli, while the seed-ROI selected in rs-fMRI is located in a purely linguistic area (triIFG), thus leading to a language network that does not include primary auditory regions. Overlap was not calculated in Case #3 since the AVG task did not provide significant activations.

Regarding the interpretation of the higher overlap between the two functional techniques in the frontal lobe compared to temporal regions, multiple factors may contribute to these findings, including the different recruitment of temporal areas in rs- and tb-fMRI as described above, the presence of temporal lobe tumors, and the broad distribution of the semantic temporal system.

In glioma patients, it might be possible that the lower overlap in the posterior regions is due to the presence of the lesions that alters the BOLD signal detected. Indeed, the highest percentage of overlap in the temporal lobe was detected for Case #1, who displayed a glioma in the superior parietal lobe, distant from the AVG activations and the resting-state functional correlations in temporal region. The overlap rate also tended to decrease based on the involvement of the temporal lobe by the tumor. Where the tumor was larger or with multifocal lesions, the percentage was lower (Case #3, #4, #5). One observation is also worthy of Case #2. Despite presenting a less extensive lesion (even if was multifocal), the patient exhibited language deficits at the time of the MR scan, differently from Case #4 and #5.

Also, reorganizational processes could have occurred and possibly have influenced the pattern of intrinsic connectivity of the language network. Given the widespread properties of cortical networks and the intrinsic nature of connectivity analysis, which assesses the degree of correlation between remote cortical areas, the presence of lesions could have impacted also on distant regions (i.e. temporal regions). As some reports demonstrated in patients with gliomas both presenting or not language deficits (Briganti et al., 2012), the presence of a brain tumor in the left hemisphere significantly reduced the degree of functional connectivity between language-related brain regions. The pattern of intrinsic connectivity was influenced by tumor position and it was not restricted to the area immediately surrounding the tumor because the connectivity between remote and contralateral areas was also affected.

An additional consideration concerning the semantic system in the temporal lobe regards its extensively described wide distribution, with distinct and task-specific roles for each functional area (Binder et al., 2009; Price, 2010). For instance, anterior temporal activation is related to semantic associations (anterior STS, lateral MTG/inferior temporal gyrus, ITG), while posterior temporal areas (MTG, ITG) are more sensitive to semantic content or increased task demands.

Limitations and future perspectives

Despite depending on an accurate and homogeneous case-selection where only patients without significant mass effect or anatomical distortions were included, it is clear that these preliminary findings should be further confirmed in a larger sample. However, our perspective in the present study was to perform single-subject evaluations, which is a topic of great interest for introducing rs-fMRI analysis in the clinical routine.

Future studies should also consider multiple language seeds, possibly selected based on the hubs identified with the IFG-derived network (e.g. the temporal seed in STG). Finally, in patients with gliomas it will be of interest to correlate fMRI data with an objective measure of cognitive deficits through the administration of a comprehensive neuropsychological battery, as well as to validate single-subject presurgical rs-fMRI networks with an intraoperative mapping using DES.

Conclusions

Our preliminary findings indicate that rs-fMRI with a seed-based correlation analysis in the IFG allows identifying the brain regions within the left fronto-temporal language networks dedicated to lexico-semantic functions in HC and patients with brain tumors, thus representing a promising tool for presurgical language mapping in glioma patients.

Although rs-fMRI-derived mapping has not been routinely employed in clinical practice yet, it has several advantages over tb-fMRI, such as the cost-effectiveness and the non-mandatory presence of on-site dedicated personnel for patient-training or task-selection. Most importantly, rs-fMRI can be exploited in non-cooperative subjects, such as cognitively-impaired patients, who may not be adequately compliant for tb-fMRI.

However, further studies on larger cohorts of tumor patients are still required to validate rs-fMRI technique in the context of preoperative planning, and to promote its growth outside academic centers.

Supplementary Material

Refer to Web version on PubMed Central for supplementary material.

Funding

The authors did not receive support from any organization for the submitted work.

Data availability

The datasets of this study is available from the authors upon request.

References

Allendorfer JB, Lindsell CJ, Siegel M, Banks CL, Vannest J, Holland SK, & Szaflarski JP (2012). Females and males are highly similar in language performance and cortical activation patterns during verb generation. Cortex; a Journal Devoted to the Study of the Nervous System and Behavior, 48(9), 1218–1233. 10.1016/j.cortex.2011.05.014 [PubMed: 21676387]

Antonsson M, Longoni F, Jakola A, Tisell M, Thordstein M, & Hartelius L (2018). Pre-operative language ability in patients with presumed low-grade glioma. Journal of Neuro-Oncology, 137(1), 93–102. 10.1007/s11060-017-2699-y [PubMed: 29196925]

Ashburner J, & Friston KJ (2005). Unified segmentation. NeuroImage, 26(3), 839–851. 10.1016/j.neuroimage.2005.02.018 [PubMed: 15955494]

Azad TD, & Duffau H (2020). Limitations of functional neuroimaging for patient selection and surgical planning in glioma surgery. Neurosurgical Focus, 48(2), E12. 10.3171/2019.11.FOCUS19769

Battistella G, Borghesani V, Henry M, Shwe W, Lauricella M, Miller Z, . . . Gorno-Tempini ML (2020). Task-Free Functional Language Networks: Reproducibility and Clinical Application. J Neurosci, 40(6), 1311–1320. 10.1523/JNEUROSCI.1485-19.2019 [PubMed: 31852732]

Battistella G, Henry M, Gesierich B, Wilson SM, Borghesani V, Shwe W, . . . Gorno-Tempini ML (2019). Differential intrinsic functional connectivity changes in semantic variant primary progressive aphasia. NeuroImage. Clinical, 22, 101797. 10.1016/j.nicl.2019.101797 [PubMed: 31146321]

Behzadi Y, Restom K, Liau J, & Liu TT (2007). A component based noise correction method (CompCor) for BOLD and perfusion based fMRI. NeuroImage, 37(1), 90–101. 10.1016/j.neuroimage.2007.04.042 [PubMed: 17560126]

Benson RR, FitzGerald DB, LeSueur LL, Kennedy DN, Kwong KK, Buchbinder BR, . . ., Rosen BR (1999). Language dominance determined by whole brain functional MRI in patients with brain lesions. Neurology, 52(4), 798–809. 10.1212/wnl.52.4.798 [PubMed: 10078731]

Berlingeri M, Crepaldi D, Roberti R, Scialfa G, Luzzatti C, & Paulesu E (2008). Nouns and verbs in the brain: Grammatical class and task specific effects as revealed by fMRI. Cognitive Neuropsychology, 25(4), 528–558. 10.1080/02643290701674943 [PubMed: 19086201]

Binder JR, Desai RH, Graves WW, & Conant LL (2009). Where is the semantic system? A critical review and meta-analysis of 120 functional neuroimaging studies. Cerebral Cortex, 19(12), 2767–2796. 10.1093/cercor/bhp055 [PubMed: 19329570]

Biswal BB, Van Kylen J, & Hyde JS (1997). Simultaneous assessment of flow and BOLD signals in resting-state functional connectivity maps. NMR in biomedicine, 10(4–5), 165–170. 10.1002/(sici)1099-1492(199706/08)10:4/5<165::aid-nbm454>3.0.co;2-7 [PubMed: 9430343]

Black DF, Vachha B, Mian A, Faro SH, Maheshwari M, Sair HI, ... Welker K (2017). American Society of Functional Neuroradiology-Recommended fMRI Paradigm Algorithms for Presurgical Language Assessment. AJNR. American journal of neuroradiology, 38(10), E65–E73. 10.3174/ajnr.A5345 [PubMed: 28860215]

Booth JR, Burman DD, Meyer JR, Gitelman DR, Parrish TB, & Mesulam MM (2003). Relation between brain activation and lexical performance. Human Brain Mapping, 19(3), 155–169. 10.1002/hbm.10111 [PubMed: 12811732]

Branco P, Seixas D, Deprez S, Kovacs S, Peeters R, Castro SL, & Sunaert S (2016). Resting-State Functional Magnetic Resonance Imaging for Language Preoperative Planning. Frontiers in Human Neuroscience, 10, 11. 10.3389/fnhum.2016.00011 [PubMed: 26869899]

Brett MA, J., Valabregue R, Poline J (2002). Region of interest analysis using an SPM toolbox [abstract]. Paper presented at the 8th International Conference on Functional Mapping of the Human Brain, Sendai, Japan

Briganti C, Sestieri C, Mattei PA, Esposito R, Galzio RJ, Tartaro A, . . . Caulo M (2012). Reorganization of functional connectivity of the language network in patients with brain gliomas. AJNR Am J Neuroradiol, 33(10), 1983–1990. 10.3174/ajnr.A3064 [PubMed: 22555573]

Buckner RL, & Vincent JL (2007). Unrest at rest: default activity and spontaneous network correlations. NeuroImage, 37(4), 1091–1099. 10.1016/j.neuroimage.2007.01.010 [PubMed: 17368915]

Cerliani L, Thomas RM, Aquino D, Contarino V, & Bizzi A (2017). Disentangling subgroups of participants recruiting shared as well as different brain regions for the execution of the verb generation task: A data-driven fMRI study. Cortex; a Journal Devoted to the Study of the Nervous System and Behavior, 86, 247–259. 10.1016/j.cortex.2016.11.017 [PubMed: 28010939]

Cirillo S, Caulo M, Pieri V, Falini A, & Castellano A (2019). Role of Functional Imaging Techniques to Assess Motor and Language Cortical Plasticity in Glioma Patients: A Systematic Review. Neural Plasticity, 2019, 4056436. 10.1155/2019/4056436 [PubMed: 31814822]

Cochereau J, Deverdun J, Herbet G, Charroud C, Boyer A, Moritz-Gasser S, Le Bars E, Molino F, Bonafé A, Menjot de Champfleur N, & Duffau H (2016). Comparison between resting state fMRI networks and responsive cortical stimulations in glioma patients. Human Brain Mapping, 37, 3721–3732. 10.1002/hbm.23270 [PubMed: 27246771]

Cole DM, Smith SM, & Beckmann CF (2010). Advances and pitfalls in the analysis and interpretation of resting-state FMRI data. Frontiers in Systems Neuroscience, 4, 8. 10.3389/fnsys.2010.00008 [PubMed: 20407579]

Cole MW, Bassett DS, Power JD, Braver TS, & Petersen SE (2014). Intrinsic and task-evoked network architectures of the human brain. Neuron, 83(1), 238–251. 10.1016/j.neuron.2014.05.014 [PubMed: 24991964]

Cordes D, Haughton VM, Arfanakis K, Carew JD, Turski PA, Moritz CH, . . . Meyerand ME (2001). Frequencies contributing to functional connectivity in the cerebral cortex in “resting-state” data. AJNR. American journal of neuroradiology, 22(7), 1326–1333 [PubMed: 11498421]

Crescentini C, Shallice T, Del Missier F, & Macaluso E (2010). Neural correlates of episodic retrieval: An fMRI study of the part-list cueing effect. NeuroImage, 50(2), 678–692. 10.1016/j.neuroimage.2009.12.114 [PubMed: 20060480]

Crinion J, Turner R, Grogan A, Hanakawa T, Noppeney U, Devlin JT, & Price CJ (2006). Language control in the bilingual brain. Science, 312(5779), 1537–1540. 10.1126/science.1127761 [PubMed: 16763154]

Doucet GE, He X, Sperling MR, Sharan A, & Tracy JI (2017). From “rest” to language task: Task activation selects and prunes from broader resting-state network. Human Brain Mapping, 38(5), 2540–2552. 10.1002/hbm.23539 [PubMed: 28195438]

Drager B, Jansen A, Bruchmann S, Forster AF, Pleger B, Zwitserlood P, & Knecht S (2004). How does the brain accommodate to increased task difficulty in word finding? A Functional MRI Study. Neuroimage, 23(3), 1152–1160. 10.1016/j.neuroimage.2004.07.005 [PubMed: 15528114]

Duffau H (2005). Lessons from brain mapping in surgery for low-grade glioma: Insights into associations between tumour and brain plasticity. Lancet Neurology, 4(8), 476–486. 10.1016/S1474-4422(05)70140-X [PubMed: 16033690]

Friederici AD, Brauer J, & Lohmann G (2011). Maturation of the language network: From inter- to intrahemispheric connectivities. PLoS ONE, 6(6), e20726. 10.1371/journal.pone.0020726 [PubMed: 21695183]

Fu CH, Morgan K, Suckling J, Williams SC, Andrew C, Vythelingum GN, & McGuire PK (2002). A functional magnetic resonance imaging study of overt letter verbal fluency using a clustered acquisition sequence: Greater anterior cingulate activation with increased task demand. NeuroImage, 17(2), 871–879. [PubMed: 12377161]

Gebska-Kosla K, Bryszewski B, Jaskolski DJ, Fortuniak J, Niewodniczy M, Stefanczyk L, & Majos A (2017). Reorganization of language centers in patients with brain tumors located in eloquent speech areas - A pre- and postoperative preliminary fMRI study. Neurologia i Neurochirurgia Polska, 51(5), 403–410. 10.1016/j.pjnns.2017.07.010 [PubMed: 28780063]

Giussani C, Roux FE, Ojemann J, Sganzerla EP, Pirillo D, & Papagno C (2010). Is preoperative functional magnetic resonance imaging reliable for language areas mapping in brain tumor surgery? Review of language functional magnetic resonance imaging and direct cortical stimulation correlation studies. Neurosurgery, 66(1), 113–120. 10.1227/01.NEU.0000360392.15450.C9

Grezes J, & Decety J (2001). Functional anatomy of execution, mental simulation, observation, and verb generation of actions: A meta-analysis. Human Brain Mapping, 12(1), 1–19. [PubMed: 11198101]

Hart MG, Price SJ, & Suckling J (2017). Functional connectivity networks for preoperative brain mapping in neurosurgery. Journal of Neurosurgery, 126(6), 1941–1950. 10.3171/2016.6.JNS1662 [PubMed: 27564466]

Hickok G, & Poeppel D (2004). Dorsal and ventral streams: A framework for understanding aspects of the functional anatomy of language. Cognition, 92(1–2), 67–99. 10.1016/j.cognition.2003.10.011 [PubMed: 15037127]

Hickok G, & Poeppel D (2007). The cortical organization of speech processing. Nature Reviews Neuroscience, 8(5), 393–402. 10.1038/nrn2113 [PubMed: 17431404]

Karnofsky DABJ (1949). Evaluation of chemotherapeutic agents (pp. pp. 191–205): MacLeod CM, editor. New York: Columbia University Press

Kosla K, Pfajfer L, Bryszewski B, Jaskolski D, Stefanczyk L, & Majos A (2012). Functional rearrangement of language areas in patients with tumors of the central nervous system using functional magnetic resonance imaging. Polish Journal of Radiology, 77(3), 39–45. [PubMed: 23049580]

Kristo G, Raemaekers M, Rutten GJ, de Gelder B, & Ramsey NF (2015). Inter-hemispheric language functional reorganization in low-grade glioma patients after tumour surgery. Cortex, 64, 235–248. 10.1016/j.cortex.2014.11.002 [PubMed: 25500538]

Lohmann G, Hoehl S, Brauer J, Danielmeier C, Bornkessel-Schlesewsky I, Bahlmann J, & Friederici A (2010). Setting the frame: The human brain activates a basic low-frequency network for language processing. Cerebral Cortex, 20(6), 1286–1292. 10.1093/cercor/bhp190 [PubMed: 19783579]

Lopes TM, Yasuda CL, Campos BM, Balthazar MLF, Binder JR, & Cendes F (2016). Effects of task complexity on activation of language areas in a semantic decision fMRI protocol. Neuropsychologia, 81, 140–148. 10.1016/j.neuropsychologia.2015.12.020 [PubMed: 26721760]

Lu J, Zhang H, Hameed NUF, Zhang J, Yuan S, Qiu T, & Wu J (2017). An automated method for identifying an independent component analysis-based language-related resting-state network in brain tumor subjects for surgical planning. Scientific Reports, 7(1), 13769. 10.1038/s41598-017-14248-5 [PubMed: 29062010]

Marien P, & Beaton A (2014). The enigmatic linguistic cerebellum: Clinical relevance and unanswered questions on nonmotor speech and language deficits in cerebellar disorders. Cerebellum & Ataxias, 1, 12. 10.1186/2053-8871-1-12 [PubMed: 26331036]

Meinzer M, Flaisch T, Wilser L, Eulitz C, Rockstroh B, Conway T, Gonzalez-Rothi L, & Crosson B (2009). Neural signatures of semantic and phonemic fluency in young and old adults. Journal of Cognitive Neuroscience, 21(10), 2007–2018. 10.1162/jocn.2009.21219 [PubMed: 19296728]

Metwali H, & Samii A (2019). Seed-Based Connectivity Analysis of Resting-State fMRI in Patients with Brain Tumors: A Feasibility Study. World Neurosurgery. 10.1016/j.wneu.2019.04.073

Muller AM, & Meyer M (2014). Language in the brain at rest: New insights from resting state data and graph theoretical analysis. Frontiers in Human Neuroscience, 8, 228. 10.3389/fnhum.2014.00228 [PubMed: 24808843]

Noll KR, Ziu M, Weinberg JS, & Wefel JS (2016). Neurocognitive functioning in patients with glioma of the left and right temporal lobes. Journal of Neuro-Oncology, 128(2), 323–331. 10.1007/s11060-016-2114-0 [PubMed: 27022915]

Oldfield RC (1971). The assessment and analysis of handedness: The Edinburgh inventory. Neuropsychologia, 9(1), 97–113. 10.1016/0028-3932(71)90067-4 [PubMed: 5146491]

Patel AX, Kundu P, Rubinov M, Jones PS, Vertes PE, Ersche KD, . . . Bullmore ET (2014). A wavelet method for modeling and despiking motion artifacts from resting-state fMRI time series. NeuroImage, 95, 287–304. 10.1016/j.neuroimage.2014.03.012 [PubMed: 24657353]

Petersen SE, Fox PT, Posner MI, Mintun M, & Raichle ME (1988). Positron emission tomographic studies of the cortical anatomy of single-word processing. Nature, 331(6157), 585–589. 10.1038/331585a0 [PubMed: 3277066]

Price CJ (2010). The anatomy of language: A review of 100 fMRI studies published in 2009. Annals of the New York Academy of Sciences, 1191, 62–88. 10.1111/j.1749-6632.2010.05444.x [PubMed: 20392276]

Price CJ (2012). A review and synthesis of the first 20 years of PET and fMRI studies of heard speech, spoken language and reading. NeuroImage, 62(2), 816–847. 10.1016/j.neuroimage.2012.04.062 [PubMed: 22584224]

Sair HI, Yahyavi-Firouz-Abadi N, Calhoun VD, Airan RD, Agarwal S, Intrapiromkul J, . . . Pillai JJ (2016). Presurgical brain mapping of the language network in patients with brain tumors using resting-state fMRI: Comparison with task fMRI. Human brain mapping, 37(3), 913–923. 10.1002/hbm.23075 [PubMed: 26663615]

Sanjuan A, Bustamante JC, Forn C, Ventura-Campos N, Barros-Loscertales A, Martinez JC, . . . Avila, C. (2010). Comparison of two fMRI tasks for the evaluation of the expressive language function. Neuroradiology, 52(5), 407–415. 10.1007/s00234-010-0667-8 [PubMed: 20177671]

Sanvito F, Caverzasi E, Riva M, Jordan KM, Blasi V, Scifo P, . . . Castellano A (2020). fMRI-Targeted High-Angular Resolution Diffusion MR Tractography to Identify Functional Language Tracts in Healthy Controls and Glioma Patients. Front Neurosci, 14, 225. 10.3389/fnins.2020.00225 [PubMed: 32296301]

Saur D, Kreher BW, Schnell S, Kümmerer D, Kellmeyer P, Vry MS, Umarova R, Musso M, Glauche V, Abel S, Huber W, Rijntjes M, Hennig J, & Weiller C (2008). Ventral and dorsal pathways for language. Proceedings of the National Academy of Sciences of the United States of America, 105(46), 18035–18040. 10.1073/pnas.0805234105 [PubMed: 19004769]

Silva MA, See AP, Essayed WI, Golby AJ, & Tie Y (2018). Challenges and techniques for presurgical brain mapping with functional MRI. Neuroimage Clin, 17, 794–803. 10.1016/j.nicl.2017.12.008 [PubMed: 29270359]

Smith SM, Fox PT, Miller KL, Glahn DC, Fox PM, Mackay CE, . . . Beckmann CF (2009). Correspondence of the brain’s functional architecture during activation and rest. Proceedings of the National Academy of Sciences of the United States of America, 106(31), 13040–13045. 10.1073/pnas.0905267106 [PubMed: 19620724]

Smitha KA, Arun KM, Rajesh PG, Thomas B, & Kesavadas C (2017). Resting-State Seed-Based Analysis: An Alternative to Task-Based Language fMRI and Its Laterality Index. AJNR. American Journal of Neuroradiology, 38(6), 1187–1192. 10.3174/ajnr.A5169 [PubMed: 28428208]

Sunaert S (2006). Presurgical planning for tumor resectioning. Journal of Magnetic Resonance Imaging, 23(6), 887–905. 10.1002/jmri.20582 [PubMed: 16649210]

Thompson-Schill SL, D’Esposito M, Aguirre GK, & Farah MJ (1997). Role of left inferior prefrontal cortex in retrieval of semantic knowledge: A reevaluation. Proceedings of the National Academy of Sciences of the United States of America, 94(26), 14792–14797. 10.1073/pnas.94.26.14792 [PubMed: 9405692]

Tomasi D, & Volkow ND (2012). Resting functional connectivity of language networks: Characterization and reproducibility. Molecular Psychiatry, 17(8), 841–854. 10.1038/mp.2011.177 [PubMed: 22212597]

Tzourio-Mazoyer N, Landeau B, Papathanassiou D, Crivello F, Etard O, Delcroix N, Mazoyer B, & Joliot M (2002). Automated anatomical labeling of activations in SPM using a macroscopic anatomical parcellation of the MNI MRI single-subject brain. NeuroImage, 15(1), 273–289. 10.1006/nimg.2001.0978 [PubMed: 11771995]

Vakamudi K, Trapp C, Talaat K, Gao K, De La Rocque Sa., Guimaraes B, & Posse S (2020). Real-Time Resting-State Functional Magnetic Resonance Imaging Using Averaged Sliding Windows with Partial Correlations and Regression of Confounding Signals. Brain Connectivity, 10(8), 448–463. 10.1089/brain.2020.0758 [PubMed: 32892629]

van den Heuvel MP, & Hulshoff Pol HE (2010). Exploring the brain network: A review on resting-state fMRI functional connectivity. European Neuropsychopharmacology, 20(8), 519–534. 10.1016/j.euroneuro.2010.03.008 [PubMed: 20471808]

Vigneau M, Beaucousin V, Herve PY, Duffau H, Crivello F, Houde O, . . . Tzourio-Mazoyer N (2006). Meta-analyzing left hemisphere language areas: phonology, semantics, and sentence processing. NeuroImage, 30(4), 1414–1432. 10.1016/j.neuroimage.2005.11.002 [PubMed: 16413796]

Vigneau M, Beaucousin V, Herve PY, Jobard G, Petit L, Crivello F, . . . Tzourio-Mazoyer N (2011). What is right-hemisphere contribution to phonological, lexico-semantic, and sentence processing? Insights from a meta-analysis. NeuroImage, 54(1), 577–593. 10.1016/j.neuroimage.2010.07.036 [PubMed: 20656040]

Weber B, Wellmer J, Schur S, Dinkelacker V, Ruhlmann J, Mormann F, . . . Fernandez G (2006). Presurgical language fMRI in patients with drug-resistant epilepsy: effects of task performance. Epilepsia, 47(5), 880–886. 10.1111/j.1528-1167.2006.00515.x [PubMed: 16686653]

Whitfield-Gabrieli S, & Nieto-Castanon A (2012). Conn: a functional connectivity toolbox for correlated and anticorrelated brain networks. Brain connectivity, 2(3), 125–141. 10.1089/brain.2012.0073 [PubMed: 22642651]

Wilson SM, Yen M, & Eriksson DK (2018). An adaptive semantic matching paradigm for reliable and valid language mapping in individuals with aphasia. Human Brain Mapping, 39(8), 3285–3307. 10.1002/hbm.24077 [PubMed: 29665223]

Yarkoni T, Poldrack RA, Nichols TE, Van Essen DC, & Wager TD (2011). Large-scale automated synthesis of human functional neuroimaging data. Nature Methods, 8(8), 665–670. 10.1038/nmeth.1635 [PubMed: 21706013]

Yuan B, Zhang N, Yan J, Cheng J, Lu J, & Wu J (2020). Tumor grade-related language and control network reorganization in patients with left cerebral glioma. Cortex; a Journal Devoted to the Study of the Nervous System and Behavior, 129, 141–157. 10.1016/j.cortex.2020.04.015 [PubMed: 32473401]

Zacà D, Jovicich J, Corsini F, Rozzanigo U, Chioffi F, & Sarubbo S (2019). ReStNeuMap: A tool for automatic extraction of resting-state functional MRI networks in neurosurgical practice. Journal of Neurosurgery JNS, 131(3), 764–771.

Zhu L, Fan Y, Zou Q, Wang J, Gao JH, & Niu Z (2014). Temporal reliability and lateralization of the resting-state language network. PLoS ONE, 9(1), e85880. 10.1371/journal.pone.0085880 [PubMed: 24475058]

Author Manuscript
Author Manuscript
Author Manuscript

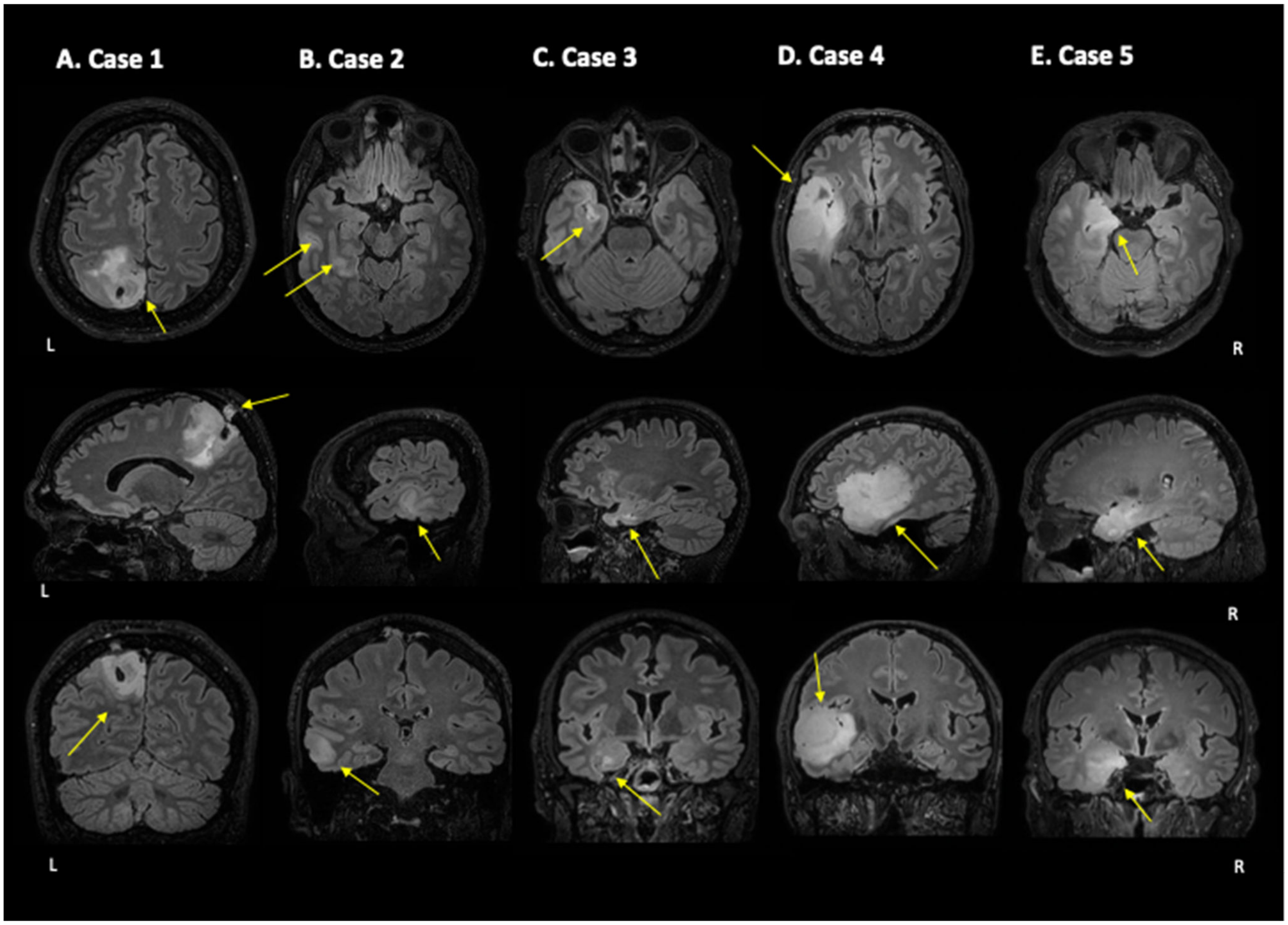

Fig. 1.
Location of left hemisphere brain tumor lesions, indicated by yellow arrows, in the five selected cases on 3D fluid attenuated inversion recovery (FLAIR) axial, sagittal and coronal sections. **(A)** Case #1: a 44-year-old female patient with an oligodendroglioma, displaying expansile, FLAIR hyperintense lesion involving both superior parietal cortex and underlying white matter as well as intratumoral hypointense signal (yellow arrow) corresponding to the previous biopsy site. **(B)** Case #2: a 46-year-old male patient with a diffuse astrocytoma, showing expansile, multifocal FLAIR hyperintense lesions located within the left middle temporal gyrus and left mesial occipito-temporal regions. **(C)** Case #3: a 34-year-old female patient with a ganglioglioma, displaying a FLAIR hyperintense, faint lesion involving the left mesial temporal lobe. **(D)** Case #4: a 48-year-old male patient with a diffuse oligodendroglioma, showing a hyperintense cortical and subcortical mass involving the left middle and superior temporal lobe and the left insula. **(E)** Case #5: a 69-year-old male patient with a glioblastoma, FLAIR MR image shows a hyperintense mass in the left mesial temporal lobe

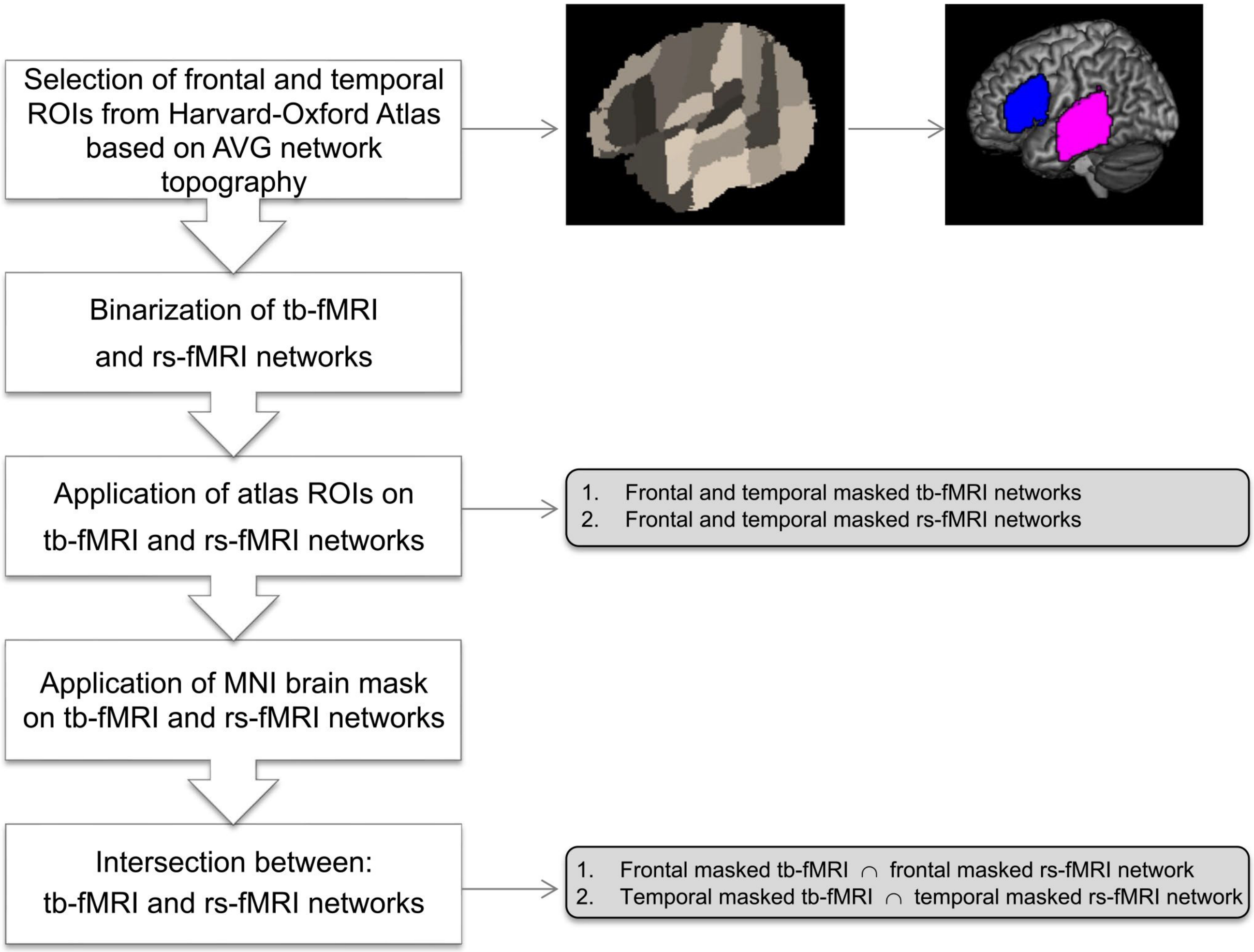

Fig. 2.
Task-based fMRI and rs-fMRI overlap analysis pipeline

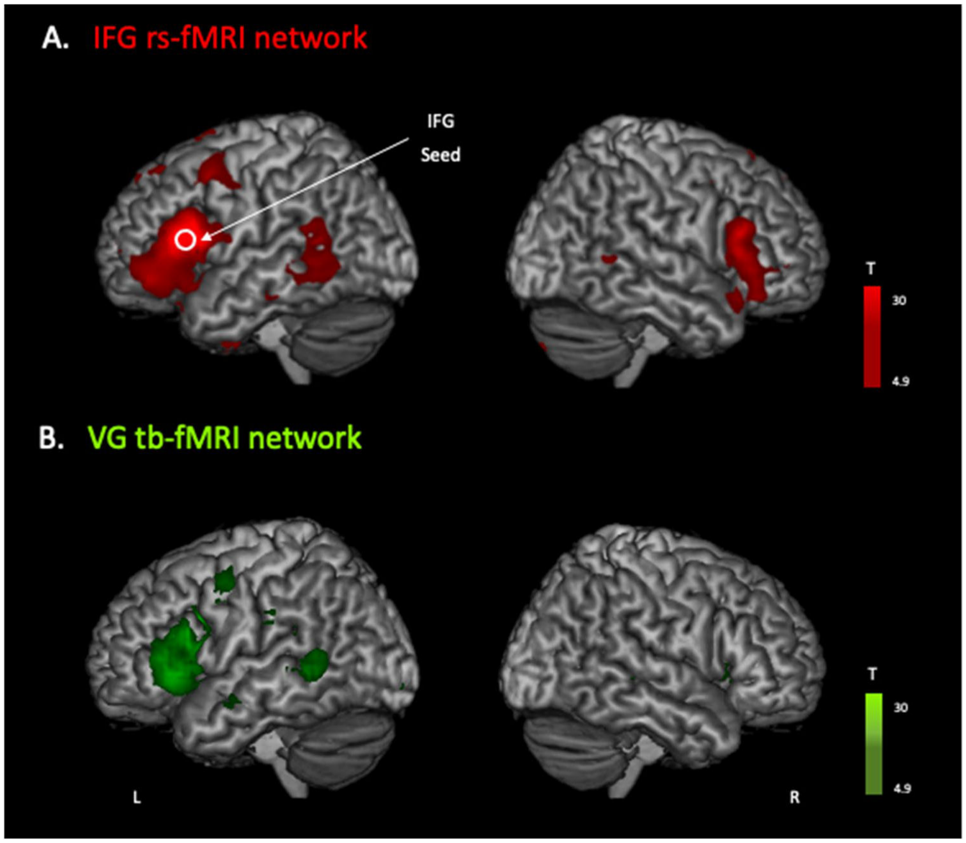

Fig. 3.

(A) Control group ICN of left triIFG ($p < 0.0001$, uncorrected T = 4.99, cluster size FWE-corrected). The white circle indicates the seed in the left triIFG [−56, 24, 15]. (**B)** Neurosynth database derived verb-generation tb-fMRI activation network ($p < 0.01$, FDR-corrected)

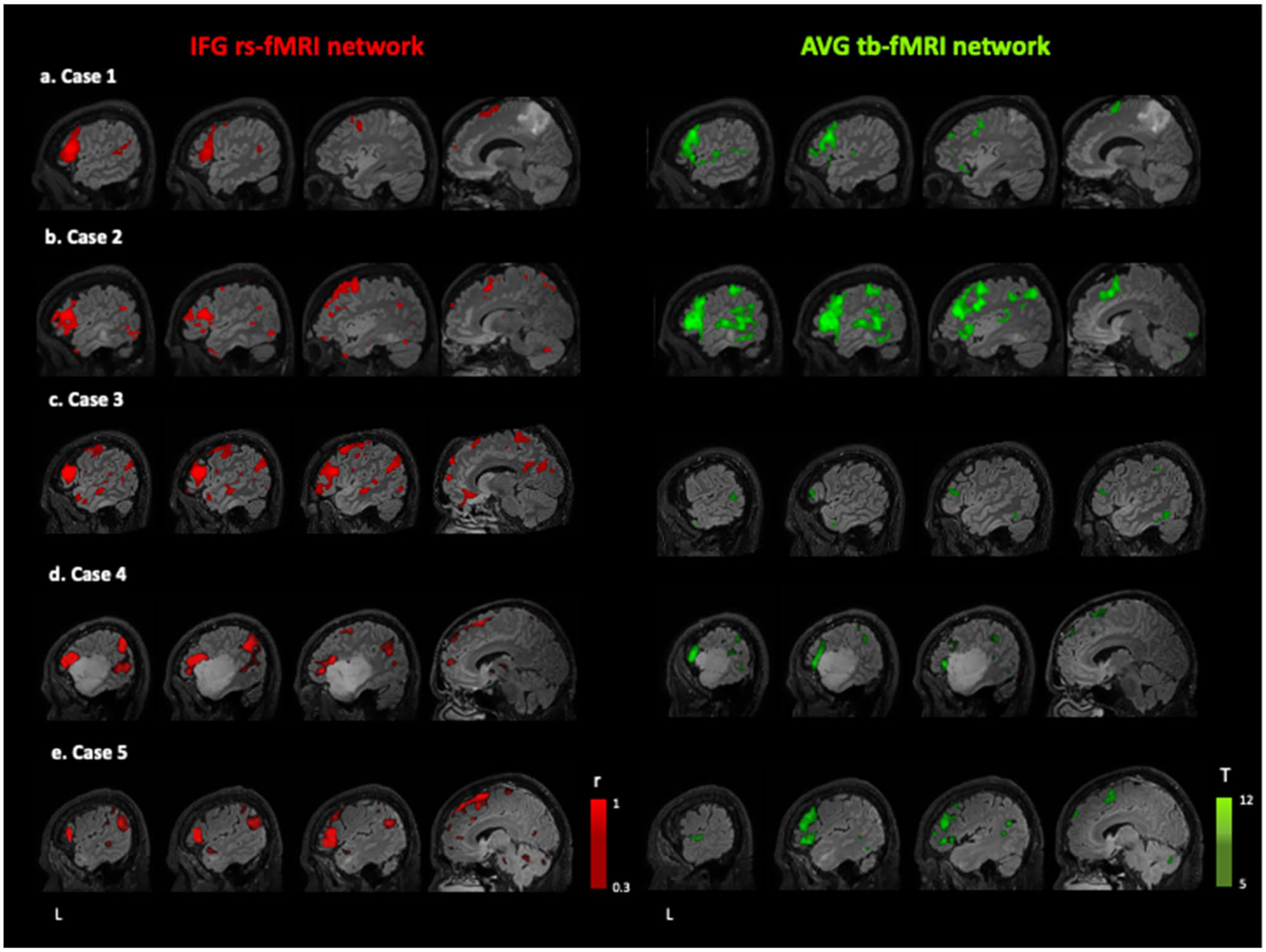

Fig. 4.

(a, b, c, d, e) Sagittal slices of subject-level rs-fMRI ICN of the triIFG on the left ($p < 0.05$; $r \geq 0.3$) and auditory verb-generation tb-fMRI in the five selected cases on the right ($p < 0.05$ FWE corrected, cluster extent > 30 voxels). **d**—Auditory verb-generation tb-fMRI for Case #3 was shown using an uncorrected threshold - ($p < 0.001$, uncorrected, cluster extent k > 10)

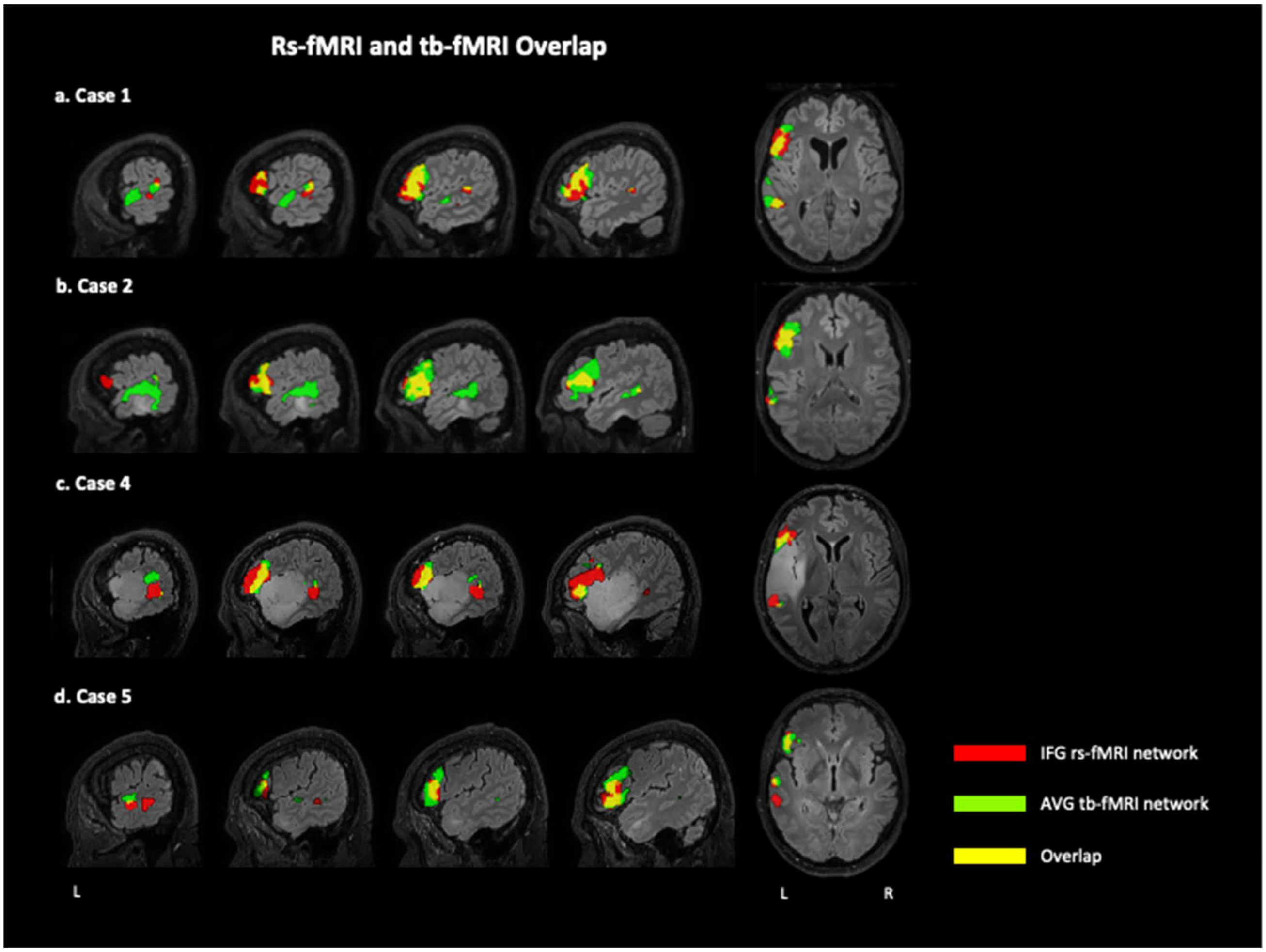

Fig. 5.

Left hemisphere overlap (yellow color) between IFG-ICN (red color) and AVG tb-fMRI (green) networks in the Case #1 **(a)**, Case #2 **(b),** Case #4 **(c)** and Case #5 **(d)**

Table 1

Patients' clinic and demographic characteristics

Case	Sex, Age	Tumor location and side	Tumor type	Grade	Clinical onset	Task	L/R[a]
#1	F, 44	L superior parietal	Oligodendroglioma	II	Loss of right arm and leg sensitivity	AVG + motor	L
#2	F, 46	L lateral and inferior temporal (multifocal)	Anaplastic astrocytoma	III	Expressive aphasia, generalized seizures	AVG, VF, PN	L
#3	F, 34	L mesial and inferior temporal	Ganglioglioma	I	Drug-resistent epilepsy	AVG, VF	L/R
#4	M, 48	L middle and superior temporal	Oligodedroglioma	III	Memory loss and right body paresthesia	AVF, VF	L
#5	M, 69	L mesial temporal	Glioblastoma	IV	Spatial-temporal disorientation and expressive aphasia	AVG, PN	L

[a]Brain lateralization was determined by clinical staff via qualitative inspection of tb-fMRI language maps

Table 2

Control group ICN of the left triIFG ($p < 0.0001$, uncorrected, T(14) = 4.99; cluster-size p-family-wise error corrected, k_min = 40)

Anatomical label AAL atlas	Side	BA	Peak MNI Coordinates	T-values	Cluster extent
IFG, pars triangularis	L	45	−56 + 22 + 16	29.8[a]	3177
IFG, pars triangularis	R	45	+ 60 + 24 + 18	12.9[a]	1298
MFG, premotor area	L	6	−42 + 10 + 48	10.2	433
STG	L	22	−66–52+14	9.2	1180
SFG, SMA/pre-SMA	L	6	−16 + 34 + 50	9.0	1048
Caudate nucleus	L	-	−14 + 06 + 18	8.3	174
Cerebellum, posterior lobe	R	-	+ 16 –76 -28	8.2	252
ITG	L	20	−36 –02 -42	8.2	164
MTG	R	21	+ 64–50 + 04	7.3	40
Caudate nucleus	R	-	+ 14 + 04 + 16	6.1	41

[a]Clusters surviving also a $p < 0.05$, family-wise error corrected for multiple comparisons

Abbreviations: AAL: Automated Anatomical Labeling BA: Brodmann area; IFG: inferior frontal gyrus; ITG: inferior temporal gyrus; MNI: Montreal Neurological Institute; MTG: middle temporal gyrus; L: left; R: right; SFG: superior frontal gyrus; STG: superior temporal gyrus